Eur. Phys. J. Plus (2022) 137:450
https://doi.org/10.1140/epjp/s13360-022-02672-0

THE EUROPEAN PHYSICAL JOURNAL PLUS

Regular Article

A new approach to studying the electrical behavior and the inhomogeneities of the Schottky barrier height

Hicham Helal[1,2,a], Zineb Benamara[1], Elisabetta Comini[2], Arslane Hatem Kacha[1], Abdelaziz Rabehi[1], Kamel Khirouni[3], Guillaume Monier[4], Christine Robert-Goumet[4], Manuel Dominguez[5]

[1] Laboratoire de Microélectronique Appliquée, Université de Sidi Bel Abbès, BP 89, 22000 Sidi Bel Abbes, Algérie
[2] Sensor Laboratory University of Brescia, Via D. Valotti 9, 25133 Brescia, Italy
[3] Laboratory of Physics of Materials and Nanomaterials Applied to the Environment, Faculty of Sciences of Gabes, University of Gabes, 6079 Erriadh City, Gabès, Tunisia
[4] Université Clermont Auvergne, Clermont Auvergne INP, CNRS, Institut Pascal, 63000 Clermont-Ferrand, France
[5] Department of Condensed Matter Physics, University of Cádiz, 11510 Puerto Real, Spain

Received: 29 September 2021 / Accepted: 1 April 2022

Abstract In this paper, two Schottky structures of Au/n-GaAs (sample A) and Au/0.8 nm-GaN/n-GaAs (sample B) were fabricated and electrically characterized by current–voltage measurements at different temperatures. Two models, a classical one and another previously proposed named Helal model ref (Helal et al. Eur Phys J Plus, 135:1–14, 2020). Both the models show that the ideality factor n grows as the temperature decreases, and the second model shows higher values especially at low temperatures. The barrier height Φ_b calculated using the second model decreases when temperature increases for both structures, according to the temperature-dependent band gap, and in contrast to the results obtained by the classical model. Moreover, the second model gives a homogeneous Schottky barrier height and the best resolution of Richardson constant A^*, for both structures. On the other hand, the classical model shows an inhomogeneity of the barrier height and very far values of A^* from the theoretical one, in both structures. The findings of this study support the validity and dependability of the proposed alternative model. Furthermore, it may give a new insight into the electrical behavior of the Schottky structures.

1 Introduction

Schottky barrier diodes (SBDs) have been widely studied in recent years due to their potential applications [1–9]. Several attempts have been performed to comprehend the electrical behavior and transport mechanisms through SBDs, in order to explain the observed phenomena. The SBDs parameters are extracted using the thermionic emission (TE) model. In this model, the barrier height strongly depends on the composition, inhomogeneity of the metallic layer [6–9], and the defects of the interface contact [10, 11]. These parameters are the main cause of the formation of the barriers height inhomogeneities. This, in turn, leads to significant increase in local current flows through different sub-regions of different resistance [12], causing the current suppressing and self-heating effects, especially at lower temperatures [11], which could lead to the burn out of the junction.

Several authors [13, 14] indicate that using the TE theory, the investigation of the I–V characteristics in GaAs-based SBDs shows nonlinearity of the Richardson characteristics [15] and an abnormal behavior of the barrier height Φ_b, since it decreases when temperature decreases in disagreement with the values of Φ_b extracted from capacitance–voltage characteristics [4–6, 9, 13, 16–20].

Researchers have already attempted to explain this finding, taking into consideration the interface state effect [21, 22], tunneling mechanisms [23–26], and the barrier inhomogeneities [27–31].

A simple common effective contact (CEC) model suggest a method to investigate the variation of the barrier height and the electrical properties with the inhomogeneous interface and the different distribution of the interfacial area [10, 32]. The weakness of the model is that there is a discrepancy between the calculated barrier heights from I-V and C-V characteristics [10].

Helal et al. [1] proposed a new model of thermionic emission mechanism with a calculating method of the electrical characteristics. They obtained a good agreement between the Φ_b derived from both *I–V* and *C–V* characteristics for different temperatures in accordance with temperature-dependent band gap. This model was validated by simulation and experimental results.

In this work, we will study the electrical behavior and Schottky barrier height inhomogeneities of two different Schottky structures, by using Helal et al. model and a classical model of *TE* current.

The tested structures are based on Au/n-GaAs and Au/0.8 nm-GaN/n-GaAs SBDs, where the *0.8 nm* nitride layer is used to passivate the GaAs surface and to eliminate the crystallographic interface dislocations, in order to improve the interface quality.

[a] e-mail: hichamwartilani@gmail.com (corresponding author)

Published online: 10 April 2022

2 Experimental part

Au/n-GaAs (sample A) and Au/0.8 nm-GaN/n-GaAs (sample B) Schottky diodes were fabricated by two different processes and electrically characterized by *I-V* measurements. The samples are based on n-GaAs substrate having a doping concentration of $N_d = 4.9 \times 10^{15}\text{cm}^{-3}$ and a thickness of 400 μm. The wafers were firstly cleaned chemically by sulfuric acid and methanol. For sample B, the n-GaAs surface were bombarded by an Ar + ion source (ion energy: 1 keV, sample current density: 5 μA cm^{-2}, time: 1 h) in the ultra-high vacuum UHV chamber. [33, 34]. Then, the wafers were nitrided using a glow discharge nitrogen plasma source, of 5 W for 30 min, and annealed at 620 °C for 1 h, in an UHV chamber [3, 35–37]. In-situ, Au dots were deposited by evaporation on the top side with a 0.6 mm diameter and 100 nm of thickness, for the two samples, using a Knudsen cell.

The *I–V* characteristics were investigated at different temperatures in the range of 140–380 K, with a Keithley 220, cooled by liquid nitrogen cryostat (Janis *VPF* 400).

3 Results and discussions

The electrical characteristics *I-V* of samples A and B are shown in Figs. 1 and 2, respectively.

For both samples, in low bias voltage, the current varies linearly versus bias voltage and shifts gradually toward the higher bias side with decreasing temperature. Then, with the increase in the bias voltage, the linearity is deviated due to the effect of the series resistance.

For ideal Schottky contacts the expression of forward *I-V* characteristics is

$$I = I_s\left[\exp\left(\frac{qV}{kT}\right) - 1\right] \tag{1}$$

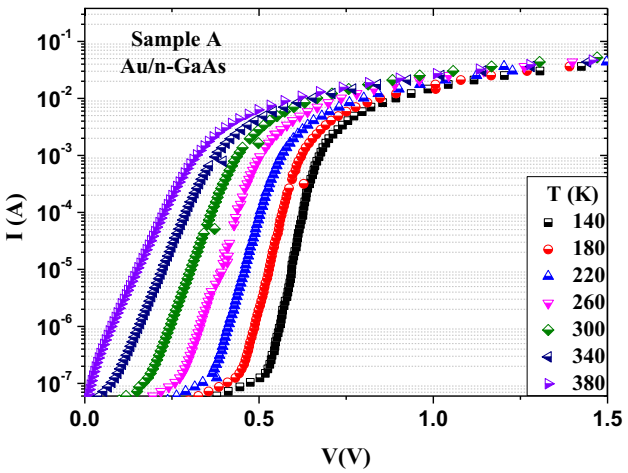

Fig. 1 *I-V-T* of sample A (Au/n-GaAs)

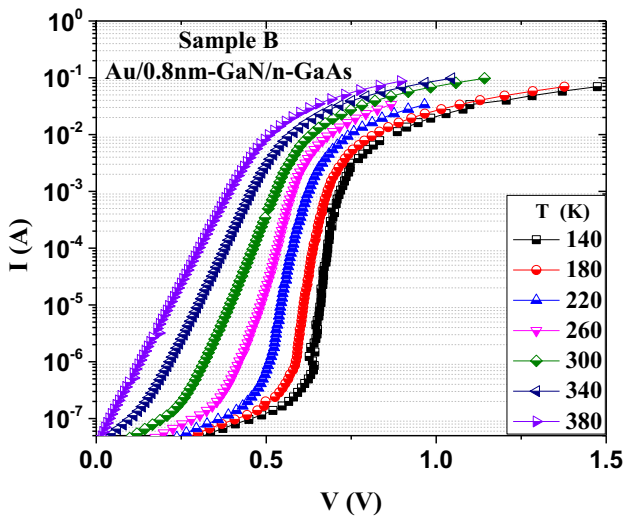

Fig. 2 *I-V-T* of sample B (Au/0.8 nm-GaN/n-GaAs)

I_s is the saturation current calculated as:

$$I_s = AA^*T^2 \exp\left(-\frac{q\Phi_b}{kT}\right) \tag{2}$$

k is the Boltzmann constant, A is the effective diode area, and A^* is the effective Richardson constant (8.16 A $cm^{-2}K^2$ for GaAs).

While, for real Schottky contacts the classical model of I-V characteristics is [38–40]:

$$I = I_s \exp\left(\frac{q(V - R_s I)}{nkT}\right) \tag{3}$$

where n and R_s are the ideality factor and series resistance, respectively.

In the Helal et al. [1] model for real Schottky contacts, it is expressed by:

$$I = AA^*T^2 exp\left(\frac{-q\Phi_b}{kT}\right) exp\left(\frac{q(V - R_s I)}{kT}\right) exp\left(-\frac{1}{n}\right) \tag{4}$$

The electrical behavior and the electrical characteristics such as n, I_s, and Φ_b are extracted and studied by the two models described by the Eqs. (3) and (4).

3.1 Extraction of the electrical parameters

3.1.1 Using the classical model

By taking into consideration that at the low bias voltage V, the current I is low, therefore the term $I R_s$ is low compared to V, Eq. (3) becomes:

$$I = I_s exp\left(\frac{qV}{nkT}\right) \tag{5}$$

and

$$ln(I) = \frac{q}{nkT} V + ln(I_s) \tag{6}$$

n and I_s are obtained from the slope and y-axis intercept of *ln(I) vs V* plot, respectively. Φ_b is determined using:

$$\Phi_b = \frac{kT}{q} ln\left(\frac{AA^*T^2}{I_s}\right) \tag{7}$$

3.1.2 Using Helal et al. model

The electrical parameters are extracted by the Helal et al. method [1] using two relationships, h_1(I) and $h_2(I)$, as follows,

$$h_1(\mathrm{I}) = \frac{\partial V}{\partial (lnI)} = \frac{nkT}{q} + R_s I \tag{8}$$

$$h_2(I) = V - \frac{KT}{q} ln\left(\frac{I}{AA^*T^2}\right) - \frac{KT}{qn} = R_s I + \Phi_b \tag{9}$$

I_s is then calculated using Eq. (2). The two methods are explained in detail in [1].

Note that the current range considered in the fit for sample A was from 1.4×10^{-7} A to 1×10^{-3} A, using classical model, and from 1.4×10^{-7} A to 3×10^{-2} A, using Helal model, for all temperatures. For sample B, it was from 4×10^{-7} A to 3×10^{-3} A, using classical model, for all temperatures, while it was from 1.4×10^{-7} A to 3×10^{-2} A for 220 K and 260 K, and from 1.4×10^{-7} A to 3×10^{-2} A for the other temperatures, using Helal model.

Figures 3 and 4 show the ideality factor n versus temperature for samples A and B, respectively, extracted by the two models.

As can be seen in these plots, for sample A (Au/n-GaAs), n increases with decreasing the temperature for both models. For sample B (Au/0.8 nm-GaN/n-GaAs), the same behavior is observed at low temperatures, while n remains almost constant and low at high temperatures (250–380 K) for the two models.

The increasing of n at low temperatures is due to the thermionic field emission *TFE* and field emission *FE* currents which became dominant instead of *TE* current [9, 13, 41]. This deviation of the transports mechanisms is more clearly defined in the Helal et al. model. This is due to the fact that in the classical model, the electrical parameters are extracted only from the linear part of the semi-logarithmic scale of the current–voltage (I-V), in the low base voltage range. In the other hand, in the Helal model, the electrical parameters are extracted from all the bias voltage for $V > 3kt/q$, and it is well known, that the ideality factor increases with increasing of the bias voltage due to the increase in the tunnel currents and the series resistance [42].

Also, the two models show low ideality factor in $T > 250$ K for the sample B, due to the nitridation of the GaAs surface which enhance the interface properties and improve the characteristics of the Schottky structure.

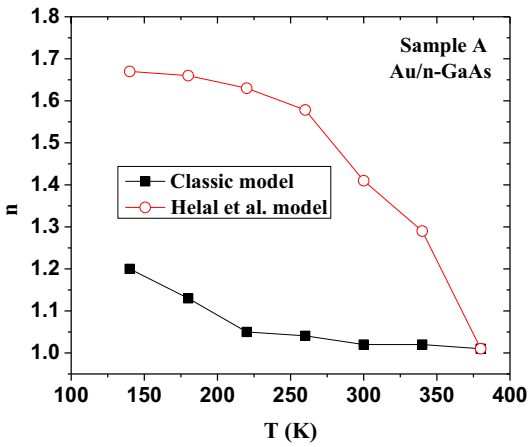

Fig. 3 n versus T for sample A

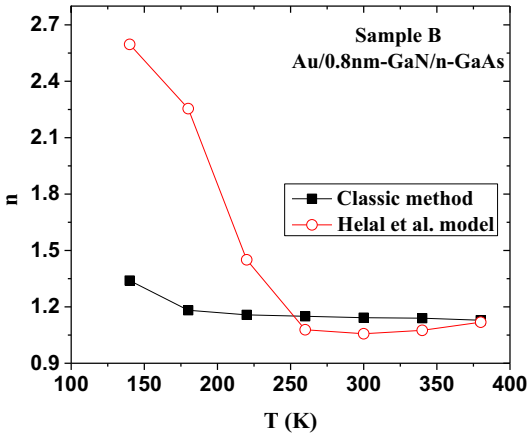

Fig. 4 n versus T for sample B

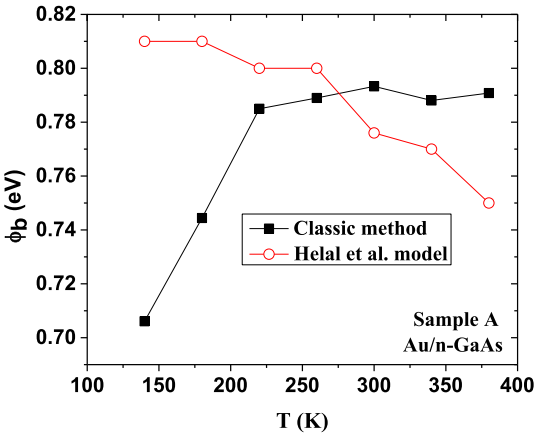

Fig. 5 Φ_b versus T for sample A

Figures 5 and 6 show the barrier height Φ_b variation versus temperature for samples A and B, respectively.

From these two figures, Φ_b extracted from the Helal et al. model decreases when temperature increases for both structures. These results confirm those previously obtained by Helal et al. [1]. As it is well known, with lowering temperature, Φ_b should grow according to the temperature-dependent band gap [13, 41, 43, 44]. On the other hand, the classical model shows the contrary, the Φ_b increases when temperature increase for sample A and it remains almost constant in the whole temperature range for sample B.

The discordance of the Φ_b obtained using the classical model and Helal model is due to the fact that classical model describe partially the current flow through the diode, and the real electrical parameters values. It is evidence by abnormal behavior of the barrier height obtained with the classical model, where it increases with increasing temperature in discordance with the band gap variation with temperature. As it is well known, with lowering temperature, Φ_b should increase according to the temperature-dependent band gap [13, 41, 43, 44]. The two models differ in the position of the ideality factor parameter in the equations. Also, in the Helal method, a wide range of current and voltage is used in the fit compared to the classical model, as mentioned before.

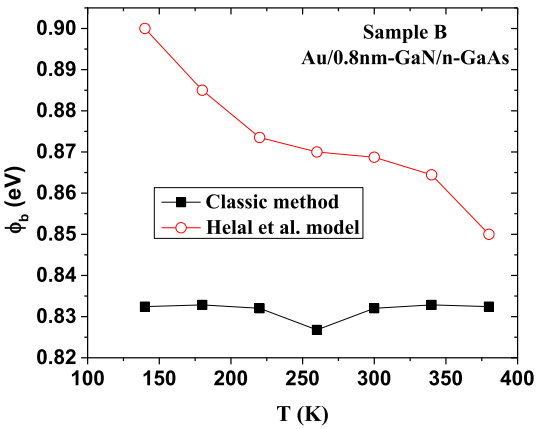

Fig. 6 Φ_b versus T for sample B

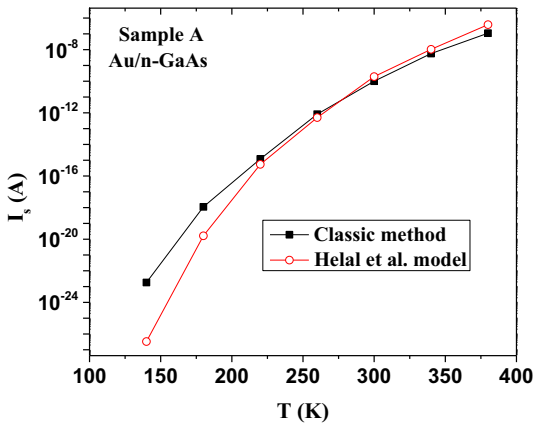

Fig. 7 I_s versus T for sample A

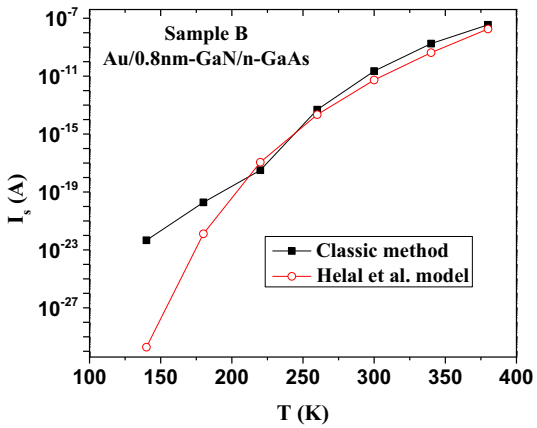

Fig. 8 I_s versus T for sample A

In addition, the Φ_b extracted from the sample B is higher than of sample A. This is due to the presence of the thin GaN layer [45].

The saturation current I_s is presented in Figs. 7 and 8 for samples A and B, respectively.

As shown in Figs. 7 and 8, the values of I_s obtained from the two models increases with increasing temperature for both samples. However, for low temperatures, the values of I_s obtained from the classical model diverges from that obtained with the model of Helal et al., and show two different forms of variation versus temperature.

Using the two models, Richardson characteristic ($ln(I_s/T^2)$ *Vs q/kT)* is used to analyze the inhomogeneity of barrier height, and is illustrated in Figs. 9 and 10 for sample A and B, respectively. Here, the following equation is used:

$$\ln\left(\frac{I_s}{T^2}\right) = \ln(AA^*) - q\frac{\Phi_{b_n}}{kT} \tag{10}$$

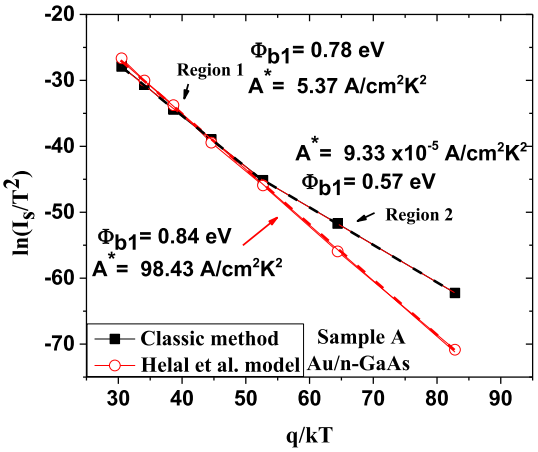

Fig. 9 $ln(I_s/T^2)$ versus q/kT for sample A

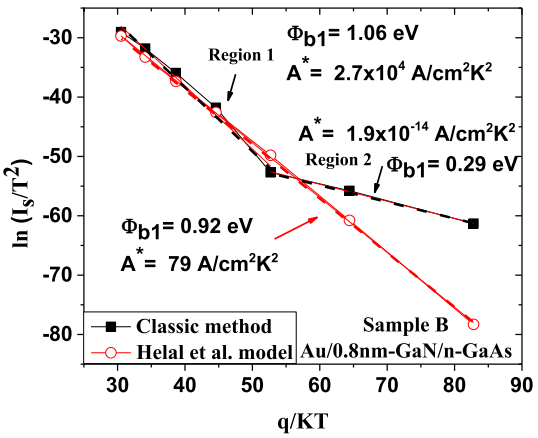

Fig. 10 $ln(I_s/T^2)$ versus q/kT for sample B

As can be seen, the Helal et al. model shows a homogeneous Schottky barrier height for both structures, since the $ln(I_s/T^2)$ versus q/kT results in a linear dependence. Parameters Φ_b and A^* were estimated at 0.84 eV and 98.43 A $cm^{-2}K^{-2}$, respectively for sample A and at 0.92 eV and 79 A $cm^{-2}K^{-2}$ respectively for sample B.

On the other hand, the classical model shows an inhomogeneity of the barrier height for both structures with two distinct regimes. For sample A, Φ_b and A^* are estimated at 0.78 eV and 5.37 A $cm^{-2}K^{-2}$ in region 1 (high temperature range), and at 0.57 eV and 9.33×10^{-5} A $cm^{-2}K^{-2}$ in region 2 (low temperature range), respectively. For sample B, Φ_b and A^* are estimated at 1.06 eV and 2.7×10^4 A $cm^{-2}K^{-2}$ in region 1 and at 0.29 eV and 1.9×10^{-14} A $cm^{-2}K^{-2}$ in region 2, respectively.

Considering the theoretical value 8.16 A $cm^{-2}K^{-2}$ of A^* for n-GaAs material and comparing the two models, it is clear that the Helal et al. model gives the best resolution and agreement, whilst the classical model shows a different behavior in two regions with some values that are very far from the expected theoretical one, and a good approximation is only shown in one region (high temperature, region 1, in sample A).

Several authors [4, 9, 18, 19, 46, 47] have found effective Richardson constant A^* values that are also very far from the theoretical one by using the classical model. This is due to the fact that the classic model is not accurate enough.

These findings support and confirm the validation and the dependability of Helal et al. model, in a wide temperature range, and show that it provides the best description of the variation of the electrical characteristics with temperature. And it gives the best approximation of the Richardson constant, which allow to the good description of the barrier height homogeneity. Also, it may give a new insight into the electrical behavior and characteristics of the Schottky structures. On the other hand, it has been shown that the classical model shows an abnormal behavior of the barrier height and gives values of the Richardson constant very far from the theoretical one, which leads to wrong description of inhomogeneity of the barrier height.

4 Conclusions

Au/n-GaAs (sample A) and Au/0.8 nm-GaN/n-GaAs (sample B) are studied in temperature range (140–380 K). The electrical parameters such as n, I_s, and Φ_b are extracted using the Helal et al. model and the classical model. The values of n obtained by the two models increases when temperature decreases in both samples, but the Helal et al. model shows higher values, especially at

low temperatures. The values of the barrier height Φ_b extracted from the Helal et al. model decreases when temperature increases for both structures, according to the variation of the band gap with temperature, in contrast to the results obtained by the classical model. Helal et al. model provides a homogeneous Schottky barrier height and the best agreement of A^* with its theoretical value, in both structures. On the other hand, the classical model shows an inhomogeneity of the barrier height and values of A^* that are far from its theoretical value in both structures. The results obtained in this work confirm the validation and the dependability of the Helal et al. model. Such model can be applied to extract real parameter values in other material junctions.

Data Availability Statements The authors declare that all other data supporting the findings of this study are available within the article.

References

1. H. Helal, Z. Benamara, B.G. Pérez, A.H. Kacha, A. Rabehi, M. Wederni, S. Mourad, K. Khirouni, G. Monier, C. Robert-Goumet, A new model of thermionic emission mechanism for non-ideal Schottky contacts and a method of extracting electrical parameters. Eur. Phys. J. Plus **135**, 1–14 (2020)
2. H. Helal, Z. Benamara, A.H. Kacha, M. Amrani, A. Rabehi, B. Akkal, G. Monier, C. Robert-Goumet, Comparative study of ionic bombardment and heat treatment on the electrical behavior of Au/GaN/n-GaAs Schottky diodes. Superlattices Microstruct. **135**, 106276 (2019)
3. H. Helal, Z. Benamara, M.A. Wederni, S. Mourad, K. Khirouni, G. Monier, C. Robert-Goumet, A. Rabehi, A.H. Kacha, H. Bakkali, Conduction mechanisms in Au/0.8 nm–GaN/n–GaAs Schottky contacts in a wide temperature range. Materials **14**, 5909 (2021)
4. H. Dogan, S. Elagoz, Temperature-dependent electrical transport properties of (Au/Ni)/n-GaN Schottky barrier diodes. Phys. E **63**, 186–192 (2014)
5. A. Kumar, S. Arafin, M.C. Amann, R. Singh, Temperature dependence of electrical characteristics of Pt/GaN Schottky diode fabricated by UHV e-beam evaporation. Nanoscale Res. Lett. **8**, 481 (2013)
6. J. Osvald, Z.J. Horvath, Theoretical study of the temperature dependence of electrical characteristics of Schottky diodes with an inverse near-surface layer. Appl. Surf. Sci. **234**, 349–354 (2004)
7. J. Osvald, J. Kuzmik, G. Konstantinidis, P. Lobotka, A. Georgakilas, Temperature dependence of GaN Schottky diodes I-V characteristics. Microelectron. Eng. **81**, 181–187 (2005)
8. S. Demirezen, E. Özavcı, Ş Altındal, The effect of frequency and temperature on capacitance/conductance–voltage (C/G–V) characteristics of Au/n-GaAs Schottky barrier diodes (SBDs). Mater. Sci. Semicond. Process. **23**, 1–6 (2014)
9. E. Özavcı, S. Demirezen, U. Aydemir, Ş Altındal, A detailed study on current–voltage characteristics of Au/n-GaAs in wide temperature range. Sens. Actuators, A **194**, 259–268 (2013)
10. T. Tuy, B. Szentpáli, I. Mojzes, The dependence of Schottky barrier height on the ratio of different metal components. Period. Polytech. Electr. Eng. (Arch.) **37**, 3–19 (1993)
11. T. Rang, Modelling of inhomogeneities of SIC Schottky interfaces. WIT Trans. Eng. Sci. **31**, 1–13 (2001)
12. R. Pascu, G. Pristavu, G. Brezeanu, F. Draghici, P. Godignon, C. Romanitan, M. Serbanescu, A. Tulbure, 60–700 K CTAT and PTAT temperature sensors with 4H-SiC Schottky diodes. Sensors **21**, 942 (2021)
13. M. Hudait, P. Venkateswarlu, S. Krupanidhi, Electrical transport characteristics of Au/n-GaAs Schottky diodes on n-Ge at low temperatures. Solid-State Electron. **45**, 133–141 (2001)
14. A. Bengi, S. Altındal, S. Özçelik, T. Mammadov, Gaussian distribution of inhomogeneous barrier height in Al0. 24Ga0. 76As/GaAs structures. Phys. B **396**, 22–28 (2007)
15. F. Padovani, G. Sumner, Experimental study of gold-gallium arsenide Schottky Barriers. J. Appl. Phys. **36**, 3744–3747 (1965)
16. S. Zeyrek, M. Bülbül, Ş Altındal, M. Baykul, H. Yüzer, The double gaussian distribution of inhomogeneous barrier heights in Al/GaN/p-GaAs (MIS) schottky diodes in wide temperature range. Braz. J. Phys. **38**, 591–597 (2008)
17. D. Korucu, A. Turut, H. Efeoglu, Temperature dependent I-V characteristics of an Au/n-GaAs Schottky diode analyzed using Tung's model. Physica B **414**, 35–41 (2013)
18. S.-Y. Lee, C.-O. Jang, J.-H. Hyung, T.-H. Kim, S.-K. Lee, High-temperature characteristics of GaN nano-Schottky diodes. Physica E **40**, 3092–3096 (2008)
19. B. Roul, T.N. Bhat, M. Kumar, M.K. Rajpalke, A. Kalghatgi, S. Krupanidhi, Analysis of the temperature-dependent current–voltage characteristics and the barrier-height inhomogeneities of Au/GaN Schottky diodes. Phys. Status Solidi (a) **209**, 1575–1578 (2012)
20. S.M. Tunhuma, F.D. Auret, M.J. Legodi, M. Diale, The effect of high temperatures on the electrical characteristics of Au/n-GaAs Schottky diodes. Phys. B **480**, 201–205 (2016)
21. J.D. Levine, Schottky-Barrier anomalies and interface states. J. Appl. Phys. **42**, 3991–3999 (1971)
22. C. Crowell, The physical significance of the T0 anomalies in Schottky barriers. Solid-State Electron. **20**, 171–175 (1977)
23. F. Padovani, *Semiconductors and semimetals*, vol. 7 (Academic Press, New York, 1971)
24. C. Crowell, V. Rideout, Normalized thermionic-field (TF) emission in metal-semiconductor (Schottky) barriers. Solid-State Electron. **12**, 89–105 (1969)
25. S. Ashok, J. Borrego, R. Gutmann, Electrical characteristics of GaAs MIS Schottky diodes. Solid-State Electron. **22**, 621–631 (1979)
26. P. Hanselaer, W. Laflere, R. Van Meirhaeghe, F. Cardon, Current-voltage characteristic of Ti-p Si metal-oxide-semiconductor diodes. J. Appl. Phys. **56**, 2309–2314 (1984)
27. S. Chand, J. Kumar, Current transport in Pd 2 Si/n-Si (100) Schottky barrier diodes at low temperatures. Appl. Phys. A **63**, 171–178 (1996)
28. Ş Karataş, Ş Altındal, A. Türüt, A. Özmen, Temperature dependence of characteristic parameters of the H-terminated Sn/p-Si (1 0 0) Schottky contacts. Appl. Surf. Sci. **217**, 250–260 (2003)
29. T. Sawada, Y. Ito, N. Kimura, K. Imai, K. Suzuki, S. Sakai, Characterization of metal/GaN Schottky interfaces based on I-V–T characteristics. Appl. Surf. Sci. **190**, 326–329 (2002)
30. J.H. Werner, H.H. Güttler, Barrier inhomogeneities at Schottky contacts. J. Appl. Phys. **69**, 1522–1533 (1991)
31. R. Tung, Electron transport at metal-semiconductor interfaces: General theory. Phys. Rev. B **45**, 13509 (1992)

32. T. Tuy, I. Mojzes, and B. Szentpáli, "The dependence of schottky barrier height of metal-semiconductor contacts on the ratio of interfacial area occupied by different metal components," in *Materials Science Forum*, pp. 101–106. (1991)
33. A. Rabehi, M. Amrani, Z. Benamara, B. Akkal, A. Hatem-Kacha, C. Robert-Goumet, G. Monier, B. Gruzza, Study of the characteristics current-voltage and capacitance-voltage in nitride GaAs Schottky diode. Eur. Phys. J. Appl. Phys. **72**, 10102 (2015)
34. A. Rabehi, M. Amrani, Z. Benamara, B. Akkal, A. Kacha, Electrical and photoelectrical characteristics of Au/GaN/GaAs Schottky diode. Optik **127**, 6412–6418 (2016)
35. G. Monier, L. Bideux, C. Robert-Goumet, B. Gruzza, M. Petit, J. Lábár, M. Menyhárd, Passivation of GaAs (001) surface by the growth of high quality c-GaN ultra-thin film using low power glow discharge nitrogen plasma source. Surf. Sci. **606**, 1093–1099 (2012)
36. H. Mehdi, F. Réveret, C. Bougerol, C. Robert-Goumet, P. Hoggan, L. Bideux, B. Gruzza, J. Leymarie, G. Monier, Study of GaN layer crystallization on GaAs (100) using electron cyclotron resonance or glow discharge N2 plasma sources for the nitriding process. Appl. Surf. Sci. **495**, 143586 (2019)
37. H. Mehdi, G. Monier, P. Hoggan, L. Bideux, C. Robert-Goumet, V. Dubrovskii, Combined angle-resolved X-ray photoelectron spectroscopy, density functional theory and kinetic study of nitridation of gallium arsenide. Appl. Surf. Sci. **427**, 662–669 (2018)
38. E. Rhoderick, R. Williams, M. S. Contacts, Oxford Science Publications, ed: Clarendon Press Oxford, (1988)
39. R. Williams, E. Rhoderick, *Metal Semiconductor Contacts*, vol. 20 (Clarendon Press, Oxford, 1988), p. 48
40. S. Sze, K.K. Ng, *Physics of Semiconductor Devices* (John Wiley and Sons Inc-2007, Hoboken, New Jersey, 2006)
41. S. Hardikar, M. Hudait, P. Modak, S. Krupanidhi, N. Padha, Anomalous current transport in Au/low-doped n-GaAs Schottky barrier diodes at low temperatures. Appl. Phys. A **68**, 49–55 (1999)
42. H. Kim, C.Y. Jung, S.H. Kim, Y. Cho, D.-W. Kim, A comparative electrical transport study on Cu/n-type InP Schottky diode measured at 300 and 100 K. Curr. Appl. Phys. **16**, 37–44 (2016)
43. R. Hackam, P. Harrop, Electrical properties of nickel-low-doped n-type gallium arsenide Schottky-barrier diodes. IEEE Trans. Electron Devices **19**, 1231–1238 (1972)
44. M. Panish, H. Casey Jr., Temperature dependence of the energy gap in GaAs and GaP. J. Appl. Phys. **40**, 163–167 (1969)
45. H. Helal, Z. Benamara, M. B. Arbia, A. Khettou, A. Rabehi, A. H. Kacha, M. Amrani, .A study of current-voltage and capacitance-voltage characteristics of Au/n-GaAs and Au/GaN/n-GaAs Schottky diodes in wide temperature range. Int. J. Numer. Modell. Electr. Netw. Dev. Fields. p. e2714 (2020)
46. D. Donoval, M. Barus, M. Zdimal, Analysis of I-V measurements on PtSi-Si Schottky structures in a wide temperature range. Solid-State Electron. **34**, 1365–1373 (1991)
47. N. Tugluoglu, S. Karadeniz, S. Acar, M. Kasap, Temperature-dependent barrier characteristics of inhomogeneous In/p-Si (100) Schottky barrier diodes. Chin. Phys. Lett. **21**, 1795 (2004)